Intermittent movement of localized excitations of a nonlinear lattice

Benno Rumpf
Max-Planck-Institute for the Physics of Complex Systems, Nöthnitzer Straße 38, 01187 Dresden, Germany
(Received 23 December 2003; revised manuscript received 4 April 2004; published 26 July 2004)

The mobility of localized high-amplitude excitations of the discrete nonlinear Schrödinger equation is studied. The excitations can either be pinned at the lattice or they can propagate depending on their energy and particle number. Such localized excitation can emit or absorb waves with a low amplitude which changes the amount of these quantities in the excitation. For statistical reasons, the excitations absorb a high amount of energy per particle through their interaction with low-amplitude waves. They can only move if their energy decreases temporarily either by a random fluctuation or by an external force.

DOI: 10.1103/PhysRevE.70.016609 PACS number(s): 42.65.Wi, 63.20.Pw, 64.60.Cn, 45.05.+x

I. INTRODUCTION

High-amplitude localized excitations that emerge spontaneously from a background of low-amplitude waves are a dynamical property of many spatiotemporal systems. Examples for this are the self-focusing of light in Kerr-nonlinear media [1], collapses in plasmas [2], and Bose-Einstein condensates [3], and possibly also the formation of extraordinarily high waves in the ocean [4]. Self-focusing behavior is a characteristic of the nonlinear Schrödinger equation and its various modifications that govern these systems. Spatially discrete systems in solid state physics [5] or molecular dynamics [6] and arrays of coupled optical fibers [7,8] can be described by ordinary differential equations such as the discrete nonlinear Schrödinger equation (DNLS):

$$i\frac{\partial \phi_n}{\partial t} = \phi_{n+1} + \phi_{n-1} + |\phi_n|^2 \phi_n \tag{1}$$

for complex amplitudes ϕ_n at sites n. Equation (1) derives as $i\dot{\phi}_n = \partial H / \partial \phi_n^*$ from the Hamiltonian (or "energy") $H = \Sigma_n (\phi_n \phi_{n+1}^* + \phi_n^* \phi_{n+1}) + 1/2\, \phi_n^2 \phi_n^{*2}$ which is a conserved quantity. The modulus-square norm (or "particle number") $A = \Sigma_n \phi_n \phi_n^*$ is a second conserved quantity of this equation. An interesting phenomenon in this spatially discrete system is the trapping of intensity peaks: High-amplitude localized solutions [9] interact most strongly with the discrete structure of the supporting medium, so that they are pinned to the lattice for most of the time and rarely migrate to a neighboring lattice site. This is shown in a simulation [Figs. 1(a) and 1(b)] where the DNLS with $N=1024$ lattice sites and periodic boundary conditions has been integrated with spatially homogeneous low-amplitude initial conditions $\phi_n(t=0)=0.3$. This homogeneous state is phase unstable, and within a few hundred time units a few high-amplitude excitations emerge from a disordered low-amplitude phonon background. The typical amplitude of an excitation is $|\phi| \approx 2$ at one central site, and with $|\phi| \approx 0.5$ at its two neighbors. The amplitudes at sites remote from these peaks are mostly below their initial values $|\phi| < 0.3$, with an exponentially decaying probability of higher amplitudes. Figure 1(a) shows the profile of the squared amplitude $|\phi_n(t)|^2$ as a function of time (from 1058 to 1073 time units after the beginning of the integration) in a small segment (11 lattice sites) of the chain. It shows the rare event of localized excitation that migrates from one lattice site to a neighboring lattice site. At first a high amount of particles (up to $|\phi_{125}|^2 \approx 4.5$) is gathered at the site 125, but at $t \approx 1066$ these particles move to the neighboring lattice site 126 within 3 time units.

The interaction with the low-amplitude waves is crucial for the migration of the peak. This interaction is studied in a second numerical experiment with Eq. (1) for a chain of 512 lattice sites [Fig. 1(c)]. The initial condition is a single isolated excitation in an environment of low-amplitude waves with a white noise spectrum. This system is integrated over 10,000 time units for various peak-heights and wave-amplitudes and it is observed whether the excitation migrates or not. Fig. 1(c) shows the time-average amplitude $|\phi|_{peak}$ of the highest localized structure that has been found to migrate at least once during the 10 000 time units of the integration as a function of the surrounding low-amplitude waves. The lattice pinning turns out to be stronger if the amplitude of the excitation is higher. The probability for a migration of a peak

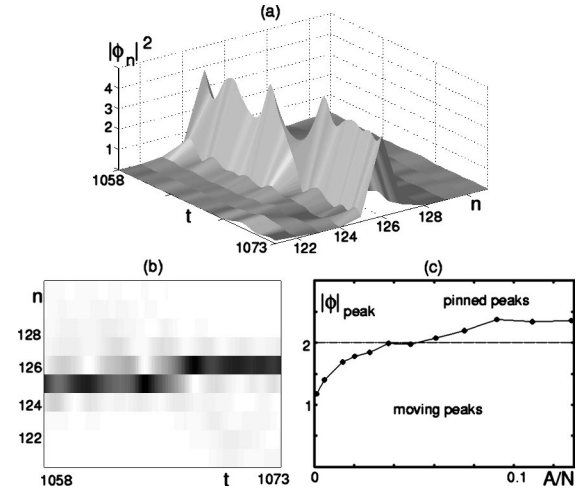

FIG. 1. (a) Particle density $|\phi_n(t)|^2$ at 11 lattice sites within a chain of 1024 lattice sites. A migration occurs during this interval of 15 time units after a long integration time. (b) The same interval in space and time as (a). Dark gray means a high particle density $|\phi_n|^2$. (c) The maximum height $|\phi_n|$ of peaks that are found to migrate as a function of the particle density A/N of the surrounding low-amplitude waves.

decreases rapidly with its height, and the threshold for the pinning of peaks is about $|\phi| \approx 2$, increasing slightly with the level of the surrounding low-amplitude waves. Peaks that are higher than the one of Figs. 1(a) and 1(b) migrate very rarely. Smaller excitations are pinned only if the surrounding waves have a very low amplitude.

The reason for this pinning effect [10–12] and its possible applications in optical signal switching [13] have been investigated in many papers. Unlike continuous systems whose solitary solutions have a Goldstone mode, solutions of discrete systems change in shape when they propagate in space. The dynamics of solitary long-wave solutions is well approximated by a continuum description, but high-amplitude excitations with a width of the order of the lattice constant are subjected to a strong spatially periodic force that impedes their movement. In a generic case where the lattice dynamics are nonintegrable, no general computation scheme for moving solutions is available. Numerically, one finds narrow solitary waves that propagate over short distances in the lattice while they radiate low-amplitude waves. Finally, they are either trapped or even disappear completely. This shows again the importance of the interaction between strongly nonlinear excitations and phonon-like waves. Stable localized solutions of the DNLS are statically pinned to the lattice. One approach to capture this feature uses the concept of the Peierls-Nabarro barrier that originally describes how the periodic lattice potential of crystals prevents the migration of defects unless some external force exceeds a threshold value. This approach [10] asserts that the migration occurs via an intermediate state with a different energy content, which requires a temporary change of the energy of the excitation. This effective pinning energy is not, however, a fixed barrier caused by the lattice because it depends also on the amplitude of the excitation itself [11]. It has been pointed out [14] that this approach assumes the conservation of the action during the migration. Alternative paths with temporarily changing amplitudes could migrate without any change of energy. Hence, the amount of particles are crucial both for the pinning and migration of localized excitations.

This paper explains the pinning and the possibility of migrations of localized excitations interacting with low-amplitude waves as a statistical process. It makes use of the recent progress of the understanding of localized solutions as statistical phenomena [15,16]. Localized excitations are considered in connection with surrounding low-amplitude waves. These waves may be described in a linear approximation, so they are sometimes referred to as phonons. Depending on the temperature of these waves, the excitations can grow or they can be melted away. This approach derives the amounts of energy and particles in the localized excitations from the thermodynamic potentials of surrounding low-amplitude waves. This explains the high density of both quantities within the excitation.

First, this paper shows that the trajectory of migrations can be described by an idealized dimer model that reduces the lattice to two sites. This migratory orbit exists only for peaks below a certain critical energy. Above this threshold, the energy conservation prevents any migration of peaks.

Second, excitations of the full lattice and their interaction with low-amplitude waves are considered. Perfect localized excitations with no surrounding low-amplitude waves are always pinned and they cannot migrate spontaneously. Migrations can be triggered, however, in the presence of surrounding of low-amplitude waves. A migration to a neighboring lattice site requires an intermediate fluctuation of the energy of the excitation that is statistically unfavorable.

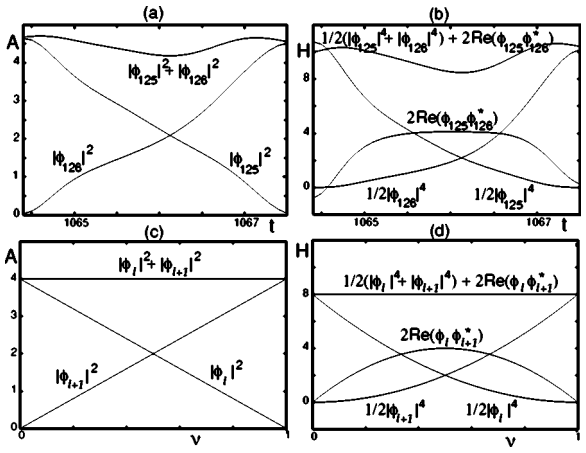

FIG. 2. Particle number $|\phi_{125}|^2$ and $|\phi_{126}|^2$ (a,c) and nonlinear energies $|\phi_{125}|^4/2$, $|\phi_{126}|^4/2$ and coupling energy $2\,\mathrm{Re}(\phi_{125}\phi^*_{126})$ (b, d) during the migration. The numerical data (a),(b) describe the migration of Figs. 1(a) and 1(b) as a function of time for $(1064.4 \leqslant t \leqslant 1067.5)$. The analytical data (c),(d) are functions of the parameter ν [see Eq. (4)].

Most figures 1(a), 1(b), 2(a), 2(b), 3(b), 6, 8, and 9 derive from one numerical simulation of a migration in Eq. (1). It has been confirmed by other similar simulations that this process of migration is representative.

II. LEVEL SETS AND THE PATH OF THE MIGRATION

A. Conservation laws during the migration

Figure 1 indicates that during the migration there is a high particle density only at the two lattice sites $n=125$, the initial location of the peak, and at $n=126$, its location after it has moved. Fig. 2(a) shows the evolution of the particle numbers at these two lattice sites during the migration. The particle number at the site 125 decreases from $|\phi_{125}|^2 \approx 4.6$ to a value close to zero. Simultaneously, the particle number at the neighboring site 126 increases from around zero to $|\phi_{126}|^2 \approx 4.5$. The total number of particles at the two sites is almost constant $|\phi_{125}|^2 + |\phi_{126}|^2 \approx 4.6 \pm 0.1$, and there is little exchange of particles between these two lattice sites and their neighbors where the amplitudes remain small during the migration. The migration is basically a transfer of particles from the "donor" lattice site 125 to the neighboring "acceptor" site 126. Corresponding to the growth and decay of the adjacent peaks, the nonlinear energy $|\phi_{126}|^4/2$ grows and $|\phi_{125}|^4/2$ decays [Fig. 2(b)]. Unlike the particle number, the sum of these two nonlinear energy contributions is not conserved and it decreases temporarily during the migration. The energy that is released from the nonlinearity is stored in the central bond so that the coupling energy $2\mathrm{Re}(\phi_{125}\phi^*_{126})$ grows temporarily [Fig. 2(b)]. The sum $|\phi_{125}|^4/2 + |\phi_{126}|^4/2$

$+2\ \mathrm{Re}(\phi_{125}\phi^*_{126})$ of the nonlinear energies at the two sites and the coupling energy in the central bond is roughly conserved.

This approximate local conservation of energy and particles at two sites suggests to model the migration process by a perfectly isolated dimer of only two oscillators ϕ_l and ϕ_{l+1}, with a constant particle number

$$A_d = |\phi_l|^2 + |\phi_{l+1}|^2 \tag{2}$$

and a constant energy that includes the nonlinear contribution from the two sites and the energy from the central bond

$$\begin{aligned} H_d &= \frac{1}{2}|\phi_l|^4 + \frac{1}{2}|\phi_{l+1}|^4 + 2\ \mathrm{Re}(\phi_l\phi_{l+1}) \\ &= \frac{1}{2}|\phi_l|^4 + \frac{1}{2}|\phi_{l+1}|^4 + 2|\phi_l||\phi_{l+1}|\cos\ \alpha, \end{aligned} \tag{3}$$

where α is the phase difference between ϕ_l and ϕ_{l+1}. This model neglects smaller fluctuations of the dimer's energy and particle content due to interactions with the surrounding low-amplitude oscillators.

B. Intersection of level sets

Writing the donor as $\phi_l = |\phi_l| e^{i(\psi+\alpha/2)}$ and the acceptor as $\phi_{l+1} = |\phi_{l+1}| e^{i(\psi-\alpha/2)}$, the four-dimensional phase space of the dimer can be represented by the three coordinates $|\phi_l|$, $|\phi_{l+1}|$, $\cos\ \alpha$, plus the trivial phase variable ψ. The two conservation laws define level sets in the phase space.

Any solution conserving Eqs. (2) and (3) is restricted to the intersection manifold of the two level sets which determines the path of the migration. Parameterized by $\nu \in [0,1]$, this onedimensional manifold is given by

$$\begin{aligned} \phi_l(\nu) &= r\sqrt{1-\nu}\, e^{i(\psi-\alpha/2)} \\ \phi_{l+1}(\nu) &= r\sqrt{\nu}\, e^{i(\psi+\alpha/2)}, \end{aligned} \tag{4}$$

with $\cos\ \alpha = r^2\sqrt{\nu-\nu^2}/2$. It connects the state $(|\phi_l(\nu=0)|=r, |\phi_{l+1}(\nu=0)|=0)$ before the migration, when all particles are gathered at the site l, and the state after the migration $[|\phi_l(\nu=1)|=0,\ |\phi_{l+1}(\nu=1)|=r]$, when all particles are gathered at $l+1$. Corresponding to the solution (4), the particle number of the initial peak $|\phi_l|^2 = r^2(1-\nu)$ decays linearly as a function of ν, while it grows as $|\phi_{l+1}|^2 = r^2\nu$ at the neighbor site [Fig. 2(c)]. Similarly, the nonlinear energies decay and grow as $r^4(1-\nu)^2/2$ and $r^4\nu^2/2$, respectively, while the bond between the two sites stores the energy $r^4(\nu-\nu^2)$ temporarily [Fig. 2(d)]. These particle and energy densities as functions of the parameter ν closely agree to the numerical data [Fig. 2(a) and 2(b)].

Figure 3(a) shows the level sets of $A_d=4$ and $H_d=8$. Their intersection set includes the initial state $|\phi_l(\nu=0)| = 2, |\phi_{l+1}(\nu=0)| = 0$.

Fig. 3(b) shows the intersection line (4) of the level sets and the trajectory of the migration of the simulation of Fig. 1. The numerical data are given as points with distances of 0.1 time units. It also shows the projections of the data to the three planes $\cos\ \alpha = 0$, $|\phi_{125}| = 0$, $|\phi_{126}| = 0$. The intersection path closely matches the numerical trajectory.

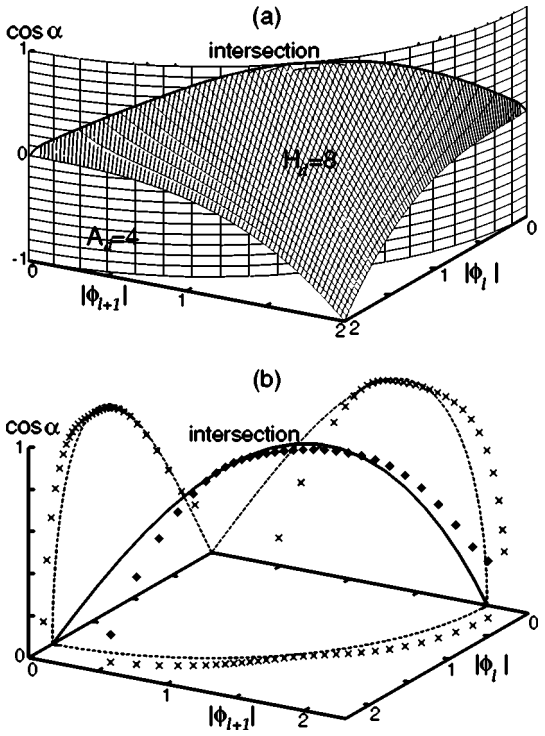

FIG. 3. (a) Level sets of A_d and H_d for a peak height $|\phi|=2.0$ as functions of $|\phi_n|$, $|\phi_{n+1}|$, $\cos\ \alpha$. (b) Intersection of the level sets for $|\phi|=2.0$ (line) and the trajectory of the peak migration from the simulation of Fig. 1 (points). The time interval is [1064.5, 1067.5], the interval between subsequent points is 0.1 time units. The dotted lines and the crosses are the projections to the level sets $|\phi|=0$ and $\cos\ \alpha = 0$.

C. Threshold of the migration

Figure 4(a) shows the intersection path that connects a donor $|\phi_l(\nu=0)|=1.5$ with an acceptor $|\phi_{l+1}(\nu=1)|=1.5$. Figure 4(b) shows that there is no such closed connection for $|\phi|=2.5$. The closed connection (4) exists only if the condition $\cos\ \alpha \leqslant 1$ is fulfilled for all $\nu \in [0,1]$. With its maximum $\cos[\alpha(\nu=1/2)] = r^2/4$ at the migration's midpoint $\nu=1/2$, this inequality is only fulfilled if $r^2 \leqslant 4$, which corresponds to an initial donor peak amplitude $|\phi(\nu=0)| \leqslant 2$.

Peaks with $|\phi| > 2$ cannot migrate, since the $|\phi|^4$-energy of the initial peak cannot be stored in the coupling term $2\ \mathrm{Re}(\phi_l\phi^*_{l+1})$ at the midpoint of the migration. It follows from the particle conservation that the amplitudes of the two oscillators are $|\phi_l(\nu=1/2)| = |\phi_{l+1}(\nu=1/2)| = r/\sqrt{2}$ at this point. Such a state of two neighboring peaks with a bond ("isolated bond" or "ib" in Fig. 5 can maximally absorb the energy $H_d = r^4/4 + r^2$ for $\alpha=0$, or a smaller amount of energy for a nonzero angle α. A single isolated peak ("ip" in Fig. 5 has an energy $H_d = r^4/2$. Figure 5 shows that the maximum energy of the central-bond state is larger than the energy of the isolated peak for $A_d < 4$ or $r < 2$. In this range a central bond state with a suitable α can absorb the energy of the initial isolated peaks. In contrast, the energy of the isolated

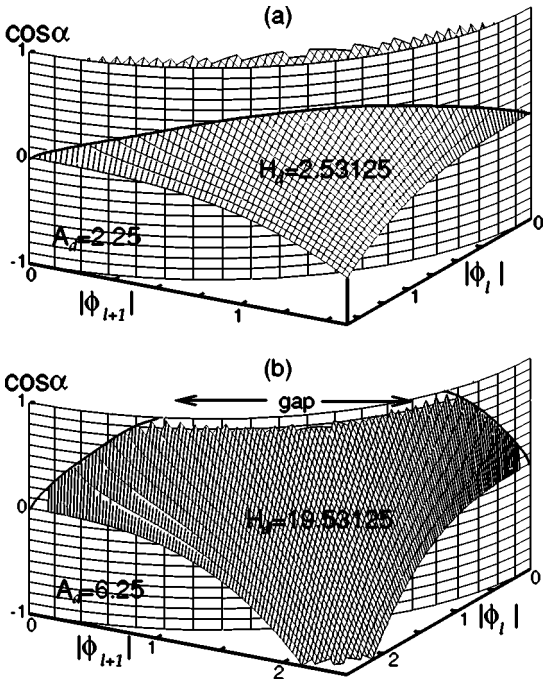

FIG. 4. Level sets of A_d and H_d for peak heights (a) $|\phi|=1.5$ and (b) $|\phi|=2.5$. For the higher initial peak (b), there is no closed connection between $|\phi_n|=2.5, |\phi_{n+1}|=0$ and $|\phi_n|=0, |\phi_{n+1}|=2.5$ on the intersection set.

peak with $A_d>4$ is higher than the energy of any intermediate central-bond state, and the local conservation laws (2) and (3) are incompatible with a migration.

The limit for large r corresponds to the original argument [10] for the Peierls-Nabarro barrier in the DNLS: For an initial donor amplitude $|\phi_l|=r$, the amplitudes of donor and acceptor will match as $|\phi_l|=|\phi_{l+1}|=r/\sqrt{2}$ at the time when half of the particles are transferred. For large r, the quadratic coupling energy can be neglected in comparison to the quartic nonlinear energy. The energy $H_d \approx r^4/4$ of this state is below the initial energy $H_d=r^4/2$, and the difference between these two energies may be regarded as a Peierls-Nabarro barrier that pins the peak at one site.

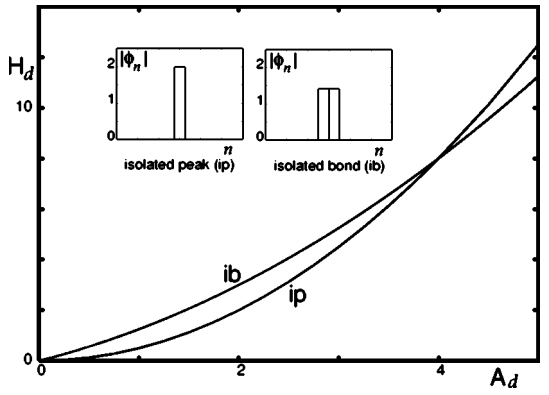

FIG. 5. Energy vs particle number of an ip and of two isolated peaks with a central bond (ib). The dimer energy of both excitations match when the particle number of the dimer is $A_d=4$.

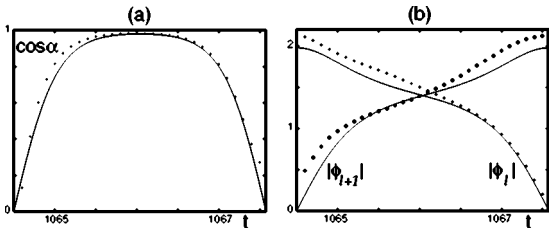

FIG. 6. (a) cos α and (b) $|\phi_l|$ and $|\phi_{l+1}|$ as functions of time during the simulation of Fig. 1 (points) and for the analytic solution of the two-site model with $r=1.96$ (lines) as functions of time.

D. Dynamics of the migration

The intersection line between the two shells $A_d=$const and $H_d=$const is an exact solution of a migration of a peak from the site l to $l+1$ in the dimer model [12,17]. Its dynamics is governed by

$$i\dot{\phi}_l = \phi_{l+1} + |\phi_l|^2\phi_l,$$
$$i\dot{\phi}_{l+1} = \phi_l + |\phi_{l+1}|^2\phi_{l+1}. \tag{5}$$

These equations are obviously integrable so that they can be solved analytically [12,17]. Equivalently they can be transformed to an equation for a particle in an effective potential [18]. The solution reproduces the intersection path of $A_d=$const and $H_d=$const as a function of time. The solution of Eq. (5) is

$$|\phi_l| = r\sqrt{[1+\mathrm{cn}(2t,r^2/4)]/2},$$
$$|\phi_{l+1}| = r\sqrt{[1-\mathrm{cn}(2t,r^2/4)]/2},$$
$$\cos\alpha = \frac{r^2}{4}\mathrm{sn}(2t,r^2/4), \tag{6}$$
$$\sin\alpha = -\mathrm{dn}(2t,r^2/4),$$

while ψ has the constant speed $\dot{\psi}=-3r^2/4$. This is exactly the intersection path (4) where $\nu(t)=\frac{1}{2}[1-\mathrm{cn}(2t,r^2/4)]$ has been determined. Figure 6 shows that $|\phi_l|$ decays monotonically from r to 0 while $|\phi_{l+1}|$ grows. cos α increases from 0 to its maximum $r^2/4$ and decays to 0 subsequently, which is only possible if the initial amplitude is $r\leqslant 2$. α grows from $-\pi/2$ to a value that is less or equal 0 and decays again to $-\pi/2$. The solution of Eq. (6) is very close (Fig. 6 where $r=1.96$) to the numerical data from the simulation of Fig. 1(a).

III. FLUCTUATIONS AND MIGRATIONS OF THE EXCITATION

The two-site model neglects all energy and particle contributions except for the donor and the acceptor site, which leads to a qualitative shortcoming of this idealized description of peak migration in the DNLS equation: The orbit (6) that connects the two excitations of the dimer is (except for $r=2$) *periodic* in time, while sufficiently high excitations of the full DNLS chain are pinned at one lattice site, before

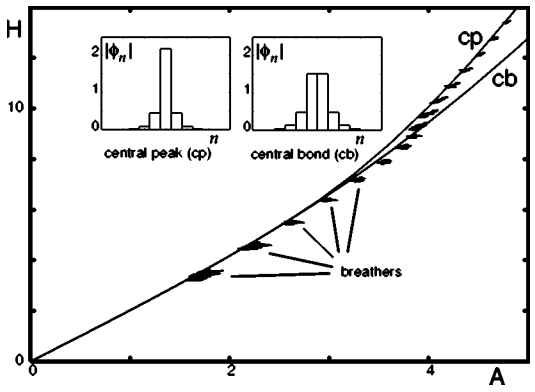

FIG. 7. Energy vs particles for the stationary central-peak (cp) solution and the central-bond (cb) solution (lines) and for breathers with various heights (points).

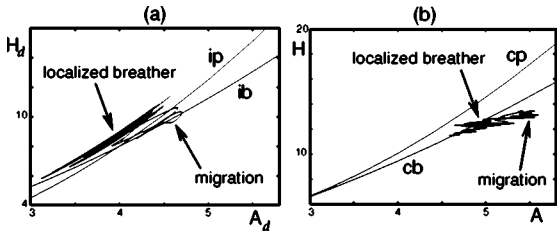

FIG. 8. Trace of the energy vs the particle number of the excitation of Fig. 1(a) over 60 time units (600 integration steps of 0.1 time units each) from $t=1035$ to $t=1095$. The migration occurs at $t\approx 1066$. (a) shows the energy and particles of only the two central lattice sites 125 and 126. (b) shows these quantities measured in a broader patch of 13 lattice sites. The lines ip, ib, cp, and cb are the same as in Figs. 5 and 7.

suddenly its particles are shifted to a neighboring lattice site where the excitation is again pinned for a long time. Real excitations are not isolated peaks at one single lattice site; they have nonzero amplitudes at neighboring lattice sites. They can absorb or emit low-amplitude waves. An investigation of the interactions between the peak and its low-amplitude environment can explain why the peak is locked at one lattice site for most of the time and why it can suddenly move to a neighboring site.

A. Stationary excitations and breathers

Excitations that are stationary in a frame rotating with the frequency ω are solutions of

$$0 = \phi_{n+1} + \phi_{n-1} + |\phi_n|^2 \phi_n + \omega \phi_n. \tag{7}$$

Reading this set of equations as a map $(\phi_{n-1}, \phi_n) \rightarrow (\phi_n, \phi_{n+1})$, localized excitations correspond to homoclinic orbits that connect the fixed point $\phi_{-\infty}=\phi_{+\infty}=0$ to itself. Equation (7) is equivalent to the condition

$$0 = \frac{\partial}{\partial \phi_n^*}(H + \omega A)$$

for extrema or saddle points of the energy where the Lagrange parameter ω constrains the particle number A.

One well-known [19] localized real solution of Eq. (7) is site centered, i.e., the amplitudes decay symmetrically at the left and the right of the site with the maximum amplitude (solution cp in Fig. 7). This central-peak solution is stable, as it has a maximum of energy for a given particle number. Central-peak solutions at different lattice sites correspond to different elliptic fixed points in phase space. There is no path that connects these islands while conserving both the energy and the particle number, and a perfect central-peak solution will not move at all.

However, some external force applied to an excitation may change its energy and move it to a neighboring lattice site. In phase space, the trajectory of such a migration corresponds to a path on which the particle number is conserved while the energy varies. The external force has to bridge the gap between the highest and the lowest energy of the excitation that migrates along this path. This energy gap is obviously different for alternative paths that connect two central-peak solutions. The smallest possible energy gap that can be found for any such path is often referred to as the Peierls-Nabarro barrier.

It is assumed [10] that this energy barrier is given by the energy difference between the central-peak solution (that defines the starting point and the end point of the path), and the solution cb in Fig. 7, which is a symmetric midpoint of the migration path. This unstable solution of Eq. (7) is a saddle point of the energy under the constraint of fixed particle number A. It has a lower energy (line cb in Fig. 7) than the site-centered solution (line cp in Fig. 7 with the same particle content, and this gap between the lines cp and cb widens with increasing values of A. It seems plausible that a path with the smallest possible change of energy will contain the central-bond solution as the intermediate state where this inevitable deviation from the initial energy is reached. Any alternative path whose energy minimum is not a saddle point could be varied in a way that reduces the energy barrier. However, the author is not aware of a formal proof for this.

This gap is smaller if the initial solution is not a stationary central-peak solution, but a solution with a similar shape and a "breathing" amplitude. Such a breather corresponds to a periodic orbit close to the elliptic fixed point of the central-peak solution. Such breather solutions have an energy slightly below the line cp. Figure 7 shows the energies and particle numbers of breathers that emerge from an initial condition with a peak at one lattice site and a zero amplitude everywhere else. The total energy of this central site and the six neighbors at its left and its right are plotted for 100 integration steps of 0.25 time units each. It turns out that breathers with particle numbers up to $A\approx 4$ have a lower energy than a central-bond solution with the same particle number, and so are more likely to migrate.

The force that causes the migration of Fig. 1 is the interaction of the localized structure with low-amplitude oscillations at neighboring sites. This interaction changes not only the energy of the moving structure, but also its particle content. Figure 8 compares the amounts of energy and particles (irregular line) in the localized excitation from Fig. 1(a) with the energy and particles of stationary central-peak and central-bond excitations. In Fig. 8(b), the amount of energy

and particles is measured in a patch of 13 lattice sites with the peak at the center in a period of 60 time units during which the migration occurs. The energy content changes relatively little compared to the particle number, which is due to the low energy of the low-amplitude waves. The energy-particle trace of the excitation is in the region of the central-bond solution (line cb), well below the line cp. The trace has to be below the line cb at least at some point of the migration, which is actually the case for much of the time. The actual migration corresponds to the largest temporary increase of the particle number, which reaches $A=5.5$ for a short period of time.

This balance concerns the total energy and particle number of the excitation. In addition to this condition, enough particles need to be available in the center of the excitation during the migration. Figure 8(a) gives the energy and particles of the donor and the acceptor site and the central bond in comparison to the lines ip and ib of the dimer of Fig. 5. At the point when the donor amplitude matches the acceptor amplitude, the energy of these two peaks and their central bond is necessarily below the line ib of Fig. 5. This is not true for most of the time and the line ib is crossed only for a short period during which the migration actually takes place. At this time, the particle number of the dimer is $A_d \approx 4.5$ [see Fig. 2(a)]. This barrier at the center of the excitation is the one that is more difficult to overcome.

B. Statistical nature of localized excitations

High-amplitude excitations like the one in Fig. 1(a) are characteristic for the long-time dynamics of the DNLS for positive energies ($H>0$) [16,20]. Virtually no oscillators have intermediate amplitudes in the range between the low-amplitude waves and the high-amplitude peaks if the particle density is small $A/N \ll 1$. The peaks are clearly distinct from the exponential tail of the low-amplitude phase. Numerical simulations show that the surrounding low-amplitude excitations have a great impact on the excitations: If their energy is positive, the excitations grow or new excitations emerge. In contrast, low-amplitude waves with a negative energy decrease the size of the excitations. On long time scales, there are no high excitations if the total energy is negative ($H<0$). In this case, the amplitude is small at all lattice sites as the probability for higher amplitudes decays exponentially. In a recent paper [16] it has been shown that this formation of localized excitations in the DNLS equation is a *statistical* phenomenon that follows from the interaction of low-amplitude waves with excitations. Those results that are important for the understanding of the pinning effect will be outlined briefly without a formal derivation. The relevant formulas from Ref. [16] are reviewed in the appendix.

The gap between the amplitudes of the excitations and the wave background suggests to describe them as two distinct physical systems. The low-amplitude waves contain a share $H_<$, $A_<$ of the energy and the particles, and may be described with a linear approximation. The peaks contain $A_>$ particles, and their energy $E_>$ is dominated by the nonlinear contribution. Excitations and linear waves can exchange particles and energy. For the statistically relevant state, the particles $A = A_< + A_>$ and energy $H = H_< + H_>$ are partitioned between the two systems so that the total entropy is maximal. The bulk of the entropy S turns out to be due to the low-amplitude waves, while the contribution from the excitations is small. The transfer of particles and energy between the two systems is related to the corresponding potentials: the chemical potential γ and the temperature β^{-1}. When the waves have a positive energy $H_<>0$, their inverse temperature β (A3) is negative. The entropy of the waves decreases as $dS/dH_< = \beta < 0$ for increasing energy of the waves. The formation of high-amplitude peaks allows the system to increase its total entropy. The energy that is released from the low-amplitude waves is absorbed by the peaks. The process stops when $H_<=0$ and $\beta=0$.

On the other hand, γ (A4) is positive for $H_<>0$, and the entropy increases with $A_<$ as $dS/dA_< = -\gamma\beta > 0$. It is therefore favorable to transfer particles from the localized excitations into the low-amplitude waves. The entropy is maximal if the waves absorb as many particles as possible, but no energy. Correspondingly, the localized structures have the highest possible ratio of energy per particle. The central-peak solution is the thermodynamically most favorable excitation because it contains more energy per particle than any other excitation. In other words, the temperature of the low-amplitude waves puts energy into the excitations, while their chemical potential extracts particles from the excitations. This thermodynamic force causes the locally high density of energy in each of the excitations. The separation of a phase of high-amplitude excitations and a phase of low-amplitude waves is the statistically most likely state only if $H>0$. For $H<0$, the formation of such peaks would decrease the entropy. Numerical experiments show that excitations are melted away in this case. This shows an interesting connection between the dynamical and the thermodynamical stability of the excitations. The central-peak solution is dynamically stable, i.e., its eigenvalues are imaginary. However, it can be destroyed by an interaction with waves with a small but finite amplitude. The thermodynamic study shows that this is the case if the waves have a negative energy. This is in agreement with numerical findings as well as with analytical computations [21] of the interaction between an excitation and a few waves. A migration of a peak is only possible if its ratio of energy per particle decreases intermediately. This can happen when the peaks exchange particles with the embedding low-amplitude waves randomly. Huge particle transfers are rare since huge fluctuations of the entropy are rare.

This explains pinning and migration of peaks as statistical processes: Depending on the gap between the lines cp and cb as well as ip and ib, fluctuations and coherent structures have to exchange particles and energy. The gap of particles between the site-centered excitation and the bond-centered excitation increases with the height of this excitation, while it is smaller for breathing peaks that have a lower energy (Fig. 7). Migrations become less likely for higher peaks as this would require an unlikely huge fluctuation in its content of particles. On the other hand, the probability of such fluctuations increases with the amplitude of the waves in the background [Fig. 1(c)].

Taking into account the fluctuations of the excitations, the migration orbit connects two tangles representing localized

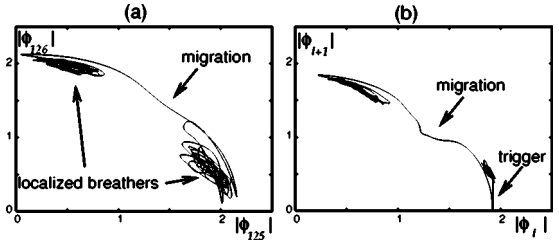

FIG. 9. (a) $|\phi_{126}|$ vs $|\phi_{125}|$ for the migration of Fig. 1(a). (b) A similar migration that is triggered by externally setting the acceptor amplitude $|\phi_{l+1}|$ to zero at one point during the numerical integration.

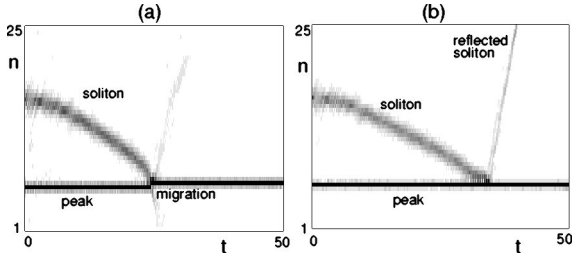

FIG. 10. (a) Collision of a peak with the height $|\phi|=1.95$ with a soliton resulting in a migration of the peak by one lattice site. (b) Collision of a peak with the height $|\phi|=2.35$ with a soliton leads to no migration.

excitations rather than perfect central-peak solutions. The migration starts when the trajectory accidentally approaches this orbit, which requires a sufficiently low energy per particle in the excitation. During the migration when $|\phi_l|$ and $|\phi_{l+1}|$ both are larger than their neighbors, this orbit is well approximated by the dimer orbit (6). As it approaches the acceptor site, the interaction with low-amplitude waves is again important and the trajectory leaves the dimer orbit. The final state is again a tangle at $l+1$. Figure 9(a) shows the trace of $(|\phi_l(t)|,|\phi_{l+1}(t)|)$ during the migration of Fig. 1(a). Before the migration, most particles are gathered at the site l with $(|\phi_l(t)|\approx 2)$, while the amplitude at $l+1$ is small and the amplitudes at both sites fluctuate irregularly. Then, following a short-lived increase of the amplitude at l, the particles migrate to $l+1$. The localized excitation is trapped at this new site until another huge fluctuation allows it to move again.

C. Trigger of migrations

Migrations can be triggered externally by setting the trajectory close to the starting point of the heteroclinic connection, rather than waiting for the system to reach this point accidentally. This is shown in Fig. 9(b) where the localized excitation rests at the site l when ϕ_{l+1} is suddenly set to zero. This reduces the energy of the central bond and the system is at the starting point of the dimer orbit (6), so that it migrates and becomes entangled at $l+1$ in a way that is similar to the migration caused by random fluctuations of Fig. 9(a).

An alternative way of triggering a migration is to change the phase of the acceptor site. The phase difference of the donor and the acceptor is $\pi/2$ at an early stage of the dimer orbit (6), while the phase difference of the central peak and its neighbors is zero for the central-peak solution cp (Fig. 7). Changing the phase of one of the neighbors by $\pi/2$ turns this site to an acceptor, so that the peak migrates. This, however, reduces the energy of the excitation after the migration.

The method also works for phase differences other than $\pi/2$, which corresponds to trajectories that are more remote from the heteroclinic orbit. For a larger phase difference, the peak can migrate over several lattice sites. The method is similar to the switching [13] of optical solitons where an external force tilts the phase by a factor $\sim\exp(-ikn)$, which also leads to a phase shift between the donor and the acceptor.

A migration can be triggered by a low-amplitude solitary wave that collides with an excitation. Figure 10 shows the impact of such collisions for peaks with two different heights. The lower peak $|\phi|\approx 1.95$ moves by one lattice site after the collision. The higher peak $|\phi|\approx 2.35$ remains at the lattice site, and the solitary wave is reflected. Due to its height, the gap between the lines ip and ib and between cb and cp are larger than the amount of particles provided by the low-amplitude soliton. The amplitude of the peak increases in either case, as both energy and particles are absorbed from the incoming soliton. The reflected or transmitted solitons carry the surplus of these quantities, therefore the collision changes their shape and speed.

Solitons have a higher density of energy and particles than waves with a low amplitude, so they have a greater impact on the excitations. They mediate the interaction of waves and excitations by transferring particles and energy. These solitons can be produced by exciting a few neighboring oscillators, and they appear spontaneously in the DNLS from a phase instability of long waves (e.g., in the simulation of Fig. 1).

These trigger mechanisms shift the peak by a few (in the earlier example only one) lattice sites, where the peak is again trapped. The reason for this is again the nonintegrable interaction of the excitation with low-amplitude oscillations. Unlike in the continuous nonlinear Schrödinger equation the DNLS has no conserved momentum, and unlike the Ablowitz-Ladik equation it has no exact soliton solutions. The trapping of moving excitations by the lattice can be seen in Fig. 11. Similarly to the process that led to the excitation of Fig. 1(a), breathers emerge at $t\approx 150$ by a phase instability of an initial low-amplitude wave $\phi_n(t=0)=0.3\exp(-ikn)$ with $k=\pi/32$. The breathers move toward higher n with a speed that is proportional to the phase tilt k of the initial condition for a few hundred time steps. At $t\approx 500$ the speed of the breathers changes erratically. At $t\approx 800$ they have merged into pinned excitation that are similar to the one of Fig. 1(a). These peaks migrate occasionally, either because they interact with solitons as in Fig. 10(a), or because of random fluctuations. The trapping of moving breathers and their merging into a few high peaks can be considered as a thermalization process where the system moves from an initial state with a low entropy to a high entropy state that is solely determined by the two conserved quantities. There is no conserved momentum of the breathers, and their speed decays by the interaction with the lattice. This interaction is strong for high, narrow excitations. A

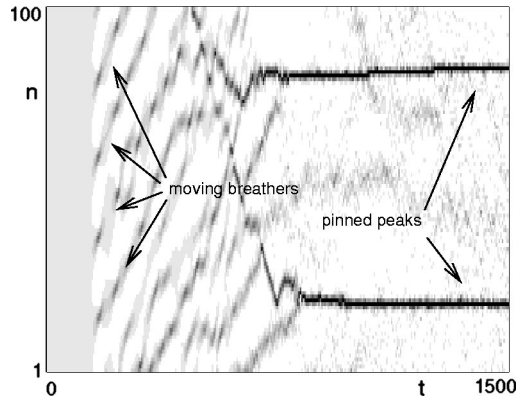

FIG. 11. Integration of the DNLS (1) with 1024 oscillators. Moving breathers emerge from a low-amplitude wave $\phi_n(t=0)=0.3e^{-i\pi n/32}$. The breathers merge into peaks with higher amplitudes that are pinned at the lattice.

moving excitation tends to grow if the surrounding low-amplitude waves have a positive energy, so that the pinning force becomes more relevant. On the other hand, it tends to decay and continues to travel if the surrounding waves have a negative energy.

IV. CONCLUSIONS

The mobility of localized excitations of the discrete nonlinear Schrödinger equation depends crucially on their interaction with low-amplitude waves. This interaction influences the amounts of energy and particles that are gathered in the excitation. An excitation can only move if it is possible to transfer these two quantities to a neighboring lattice site in a continuous process.

The energy and particle balance of migrations has been considered in two different ways, first, only for the two sites (donor and acceptor) that have the highest amplitude during the migration, second, for the broader structure of the excitation including adjacent sites with lower amplitudes. Figure 2 shows that energy and particles are almost conserved during the migration process for the simple model of only two sites. From this, a threshold $|\phi|=2$ (Fig. 5) for the maximum height of moving excitations can be derived. The trajectory of the migration can be computed analytically (Fig. 3) below this threshold, while there is no such trajectory beyond this threshold (Fig. 4).

Excitations in numerical experiments resemble the central-peak solution of Fig. 7 more than the isolated peak of Fig. 5. This can be explained statistically: The DNLS is a nonintegrable dynamical system in which the excitations can absorb or emit low-amplitude waves. Excitations and low-amplitude waves coexist in the equilibrium state where the entropy is maximal [16]. The entropy is maximal when the low-amplitude waves contain as many particles as possible, but no energy. Correspondingly, the excitations absorb the total energy using a minimum amount of particles. The central-peak excitations of Fig. 7 have the highest possible ratio of energy per particle and are thermodynamically stable if the system's total energy is positive. The interaction with low-amplitude waves forces the excitation into a state that is close to this solution. This excitation is usually pinned at the lattice since no path conserving both energy and particles connects such an excitation with a similar excitation at neighboring lattice sites.

Only if an external force changes the local particle number or energy temporarily can the excitation move. Interestingly, one possible cause for this is again the excitation's interaction with low-amplitude waves. While this causes a high ratio of energy per particle in the excitation on average, it also leads to fluctuations on short time scales. This allows the excitation to move if its energy decays below the energy of a central bond solution (Fig. 7). In other words, while the interaction with the waves is responsible for the pinning of the excitation, it can have the opposite effect when sporadic huge fluctuations trigger a migration. After moving over one or a few lattice sites, the excitation is again trapped at its new location as the interaction with the waves increases its energy again. If the waves have a negative energy, the excitation will rather decrease in size and continue to move.

The pinning effect explains the numerical finding of maximum amplitudes slightly above $|\phi|=2$ in long-time simulations with low-amplitude initial conditions. The entropy would increase if these peaks merged into a smaller number of higher peaks. However, this does not happen on realistic time scales since migrations of these excitations are rare enough that fusions of pinned peaks are excluded (Fig. 11).

External forces can be used to trigger a migration in a similar way. Three mechanisms for this have been discussed: Either, the phase or the amplitude of the acceptor can be changed, or a low-amplitude soliton can collide with the excitation. The main point of these switching mechanisms is that they decrease the ratio of energy per particle and that they set the trajectory close to the heteroclinic connection between the donor and the acceptor site.

APPENDIX: THERMODYNAMIC EQUILIBRIUM OF THE DISCRETE NONLINEAR SCHRÖDINGER EQUATION

A statistical description of the equilibrium state of the discrete nonlinear Schrödinger equation [16] is based on the grand partition function

$$y(\beta,\gamma)=\int e^{-\beta(H-\gamma A)}d\Gamma, \tag{A1}$$

where the two parameters β and γ reflect the conservation of H and A. An analytic approximation of this can be computed in the case of a low particle density. For any solution with a low particle density $\langle|\phi_n|^2\rangle=A/N\ll 1$, the amplitude has to be small $|\phi_n|\sim\mathcal{O}\sqrt{A/N}$ at almost all lattice sites. High amplitudes $|\phi_n|\gg\sqrt{A/N}$ will occur at very few sites. For instance, the number of sites with amplitudes $|\phi|\sim\mathcal{O}(1)$ is at most proportional to $A\ll N$. At the sites where the amplitude is small, the quartic energy contribution $|\phi_n|^4/2$ will be negligible compared to quadratic contribution $\phi_n\phi_{n+1}^*+\phi_n^*\phi_{n+1}$. On the other hand, the quartic contribution will prevail at high-amplitude sites.

This suggests to simplify the Hamiltonian by neglecting the quartic energy contribution for low-amplitude excitations, and by neglecting the coupling energy for the high peaks. Introducing the border $r \gg \sqrt{A/N}$ between "high" and "low" amplitudes, the Hamiltonian can be approximated by the sum $H \approx H_< + H_>$ of a low-amplitude contribution

$$H_< = \sum_{|\phi_n|,|\phi_{n+1}|<r} \phi_n \phi_{n+1}^* + \phi_n^* \phi_{n+1}$$

and a high-amplitude contribution

$$H_> = \sum_{|\phi_n|>r} |\phi_n|^4/2.$$

Similarly, the particle number is divided in two components as $A = A_< + A_>$.

Using this separation of the energy and the particle number, the integration of Eq. (A1) can be carried out in the high- and low-amplitude domain separately. The low-amplitude phase and the peaks are two thermodynamic systems that are coupled by their common temperature β^{-1} and the chemical potential γ since particles and energy can be exchanged between the peaks and the waves. The canonic transformation $S(H,A) = \ln y + \beta(H - \gamma A)$ yields the leading term of the entropy

$$S \approx N \ln \Omega \tag{A2}$$

with $\Omega = (4A_<^2 - H_<^2)/(4A_< N)$. This predominant contribution to the entropy is due to the low-amplitude waves. The peaks' contribution to the entropy turns out to be negligible, but they can absorb high amounts of energy. The inverse temperature is

$$\beta = -\frac{2H_< N}{4A_<^2 - H_<^2} \tag{A3}$$

and the chemical potential is

$$\gamma = \frac{4A_<^2 + H_<^2}{2H_< A_<}. \tag{A4}$$

The entropy is maximal for $H_< \approx 0$, $H_> \approx H$, $A_< \approx A$, $A_> \approx 0$. This corresponds to a single high peak that absorbs all the energy, while the low-amplitude waves have a white power spectrum and absorb all particles.

[1] P. L. Kelley, Phys. Rev. Lett. **15**, 1005 (1965).
[2] V. E. Zakharov, Zh. Eksp. Teor. Fiz. **62**, 1759 (1972) [Sov. Phys. JETP **35**, 908 (1972)].
[3] F. Dalfovo, S. Giogini, L. P. Pitaevskii, and S. Stringari, Rev. Mod. Phys. **71**, 463 (1999).
[4] M. Onorato, A. R. Osborne, M. Serio, and S. Bertone, Phys. Rev. Lett. **86**, 5831 (2001).
[5] B. I. Swanson, J. A. Brozik, S. P. Love, G. F. Strouse, A. P. Shreve, A. R. Bishop, W.-Z. Wang, and M. I. Salkola, Phys. Rev. Lett. **82**, 3288 (1999); R. Morandotti, U. Peschel, J. S. Aitchison, H. S. Eisenberg, Y. Silberberg, *ibid.* **83**, 2726 (1999).
[6] M. Peyrard, Nonlinearity **17**, R1 (2004).
[7] H. S. Eisenberg, Y. Silberberg, R. Morandotti, A. R. Boyd, and J. S. Aitchison, Phys. Rev. Lett. **81**, 3383 (1998).
[8] A. B. Aceves, C. De Angelis, G. G. Luther, A. M. Rubenchik, and S. K. Turitsyn, Physica D **87**, 262 (1995); A. B. Aceves, C. DeAngelis, T. Peschel, R. Muschall, F. Lederer, S. Trillo, and S. Wabnitz, Phys. Rev. E **53**, 1172 (1996).
[9] A. J. Sievers and S. Takeno, Phys. Rev. Lett. **61**, 970 (1988).
[10] Y. S. Kivshar and D. K. Campbell, Phys. Rev. E **48**, 3077 (1993).
[11] S. Flach and C. R. Willis, Phys. Rev. Lett. **72**, 1777 (1994).
[12] S. Aubry, G. Kopidakis, A. M. Morgante, and G. P. Tsironis, Physica B **296**, 222 (2001).
[13] R. A. Vicencio, M. I. Molina, and Y. S. Kivshar, Opt. Lett. **28**, 1942 (2003); http://arxiv.org/abs/physics/0401089.
[14] R. S. MacKay and S. Aubry, Nonlinearity **7**, 1623 (1994).
[15] B. Rumpf and A. C. Newell, Phys. Rev. Lett. **87**, 054102 (2001); B. Rumpf and A. C. Newell, Phys. Rev. E **69**, 026306 (2004).
[16] B. Rumpf, Phys. Rev. E **69**, 016618 (2004).
[17] V. M. Kenkre and D. K. Campbell, Phys. Rev. B **34**, 4959 (1986).
[18] M. I. Molina and G. P. Tsironis, Int. J. Mod. Phys. B **9**, 1899 (1995); W. D. Deering and M. I. Molina, IEEE J. Quantum Electron. **33**, 336 (1997); M. I. Molina, Mod. Phys. Lett. B **13**, 225 (1999).
[19] J. Carr and J. C. Eilbeck, Phys. Lett. **109A**, 201 (1985).
[20] B. Rumpf and A. C. Newell, Physica D **184**, 162 (2003).
[21] M. Johansson, Phys. Rev. E **63**, 037601 (2001).